Therapeutic Implications of a Human Neutralizing Antibody to the Macrophage-Stimulating Protein Receptor Tyrosine Kinase (RON), a c-MET Family Member

Jennifer M. O'Toole,[1] Karen E. Rabenau,[1] Kerri Burns,[1] Dan Lu,[2] Venkat Mangalampalli,[3] Paul Balderes,[4] Nicole Covino,[4] Rajiv Bassi,[5] Marie Prewett,[5] Kimberly J. Gottfredsen,[6] Megan N. Thobe,[7] Yuan Cheng,[1] Yiwen Li,[5] Daniel J. Hicklin,[5] Zhenping Zhu,[2] Susan E. Waltz,[7] Michael J. Hayman,[6] Dale L. Ludwig,[3] and Daniel S. Pereira[1]

Departments of [1]Tumor Biology, [2]Antibody Engineering, [3]Cell Engineering and Expression, [4]Protein Sciences, and [5]Experimental Therapeutics, ImClone Systems, Inc.; [6]Department of Molecular Genetics and Microbiology, SUNY at Stonybrook, New York, New York; and [7]Department of Surgery, University of Cincinnati College of Medicine, Cincinnati, Ohio

Abstract

RON is a member of the c-MET receptor tyrosine kinase family. Like c-MET, RON is expressed by a variety of epithelial-derived tumors and cancer cell lines and it is thought to play a functional role in tumorigenesis. To date, antagonists of RON activity have not been tested *in vivo* to validate RON as a potential cancer target. In this report, we used an antibody phage display library to generate IMC-41A10, a human immunoglobulin G1 (IgG1) antibody that binds with high affinity (ED_{50} = 0.15 nmol/L) to RON and effectively blocks interaction with its ligand, macrophage-stimulating protein (MSP; IC_{50} = 2 nmol/L). We found IMC-41A10 to be a potent inhibitor of receptor and downstream signaling, cell migration, and tumorigenesis. It antagonized MSP-induced phosphorylation of RON, mitogen-activated protein kinase (MAPK), and AKT in several cancer cell lines. In HT-29 colon, NCI-H292 lung, and BXPC-3 pancreatic cancer xenograft tumor models, IMC-41A10 inhibited tumor growth by 50% to 60% as a single agent, and in BXPC-3 xenografts, it led to tumor regressions when combined with Erbitux. Western blot analyses of HT-29 and NCI-H292 xenograft tumors treated with IMC-41A10 revealed a decrease in MAPK phosphorylation compared with control IgG–treated tumors, suggesting that inhibition of MAPK activity may be required for the antitumor activity of IMC-41A10. To our knowledge, this is the first demonstration that a RON antagonist and specifically an inhibitory antibody of RON negatively affects tumorigenesis. Another major contribution of this report is an extensive analysis of RON expression in ~100 cancer cell lines and ~300 patient tumor samples representing 10 major cancer types. Taken together, our results highlight the potential therapeutic usefulness of RON activity inhibition in human cancers. (Cancer Res 2006; 66(18): 9162-70)

Introduction

The macrophage-stimulating protein receptor (RON) belongs to the c-MET family of receptor tyrosine kinases (1–3). RON ligand, macrophage-stimulating protein (MSP), was originally found to modulate the function of certain macrophage by a variety of means. For example, addition of MSP not only induced shape changes, chemotaxis, macropinocytosis, and phagocytosis (4) but also inhibited lipopolysaccharide (LPS)-induced production of inflammatory mediators such as inducible nitric oxide (5), nitric oxide (6), prostaglandins, and cyclooxygenase-2 (7). Consistent with this notion that RON negatively regulates inflammation is the observation that activated macrophages from adult RON knockout mice produced increased levels of nitric oxide both *in vitro* and *in vivo*, thus rendering them more susceptible to LPS-induced endotoxic shock (8–10). Besides macrophage, RON has also been found expressed in several normal epithelial cells such as keratinocytes (11) where MSP was shown to phosphorylate RON and activate a number of signaling pathways that elicited cell adhesion/motility and antiapoptotic and proliferative responses (12).

As is the case with its better-known family member, c-MET, several lines of evidence suggest a role for RON in cancer. First, it is highly expressed in several epithelial tumors and cell lines of the colon (13), lung (14), breast (15, 16), stomach (17), ovary (18), pancreas (3), bladder (19), liver (20), and kidney (21, 22). RON is also found coexpressed in tumors with other growth factor receptors such as c-MET and epidermal growth factor receptor (EGFR; refs. 16, 19, 23, 24). Second, MSP and RON have been shown to influence the migration and invasion of cancer cells (2, 3, 25). Third, the oncogenic potential of RON has been shown on overexpression in cultured cell lines (26–28) and in transgenic mice (29, 30) where overexpression of RON led to a profound increase in proliferation and tumorigenesis, respectively. Down-regulation of RON expression in RON-expressing cancer cell lines resulted in a reduction in proliferation (31). Similar oncogenic potential has also been observed for splice variants of RON identified in tumors and cell lines that generate receptors completely lacking the extracellular domain or that harbor deletions within this domain (26, 27, 32–35). Fourth, RON synergizes with known oncogenes. For example, the skin and breast tumorigenicity of transgenic mice overexpressing the polyoma middle T (36) and RAS (37) oncogenes, respectively, is repressed when these mice are crossed to RON knockout mice.

Whereas several antagonists of c-MET have shown antitumor activity and thus validated c-MET as a cancer target, to date, antagonists of RON activity have not shown antitumor activity to validate RON as a potential cancer target. Consequently, through the screening of a human Fab phage display library, we developed IMC-41A10, a human IgG1 monoclonal antibody that binds with

Note: Supplementary data for this article are available at Cancer Research Online (http://cancerres.aacrjournals.org/).

J.M. O'Toole and K.E. Rabenau contributed equally to this work.

Requests for reprints: Daniel S. Pereira, Department of Tumor Biology, ImClone Systems, Inc., 180 Varick Street, New York, NY 10014. Phone: 646-638-5008; Fax: 212-645-2054; E-mail: daniel.pereira@imclone.com.

doi:10.1158/0008-5472.CAN-06-0283

high affinity to human RON and blocks MSP binding. In RON-expressing cancer cell lines, we show IMC-41A10 to be a potent inhibitor of receptor signaling, cell migration, and tumorigenesis. To our knowledge, this is the first demonstration of a RON antagonist, and specifically an inhibitory antibody of RON, that negatively affects tumorigenesis. Another major contribution of this report is an extensive analysis of RON expression in ~100 cancer cell lines and ~300 patient tumor samples representing 10 and 6 major cancer types, respectively. Taken together, our results underscore the potential therapeutic usefulness of RON activity inhibition in human neoplasia.

Materials and Methods

Immunohistochemistry. The polyclonal RON (C-20) antibody from Santa Cruz Biotechnology (Santa Cruz, CA), which has previously been used to detect RON expression by immunohistochemistry (17), was used here to detect RON expression in breast (51 samples, IMH-364), lung (59 samples, IMH-305), prostate (40 samples, IMH-303), stomach (59 samples, IMH-316), and colon (59 samples, IMH-306) tumor tissue arrays purchased from Imgenex (Sorrento Valley, CA). Pancreatic tumor tissue arrays (54 samples, CC1401) were obtained from Cybrdi (Frederick, MD). These formalin-fixed paraffin-embedded arrays were treated and stained with 1.2 μg/mL RON (C-20) antibody or rabbit IgG as a negative control (Jackson Immuno-Research Laboratories, West Grove, PA) using the EnVision+ Rabbit Kit (DAKO, Carpinteria, CA) as described (38).

Cell culture. Cell lines used in this study were obtained from the American Type Culture Collection (Manassas, VA) and grown exactly as recommended. Media used for their propagation were purchased from Life Technologies, Inc. (Grand Island, NY).

Flow cytometry. To measure cell-surface expression of RON, cancer cell lines were grown to subconfluence, trypsinized, washed, pelleted (5 minutes, 1,400 rpm), and resuspended/filtered in 250 μL PBS + 5% fetal bovine serum (FBS). Five micrograms of RON antibody (IMC-41A10) were added to all tubes, except the control tube, and incubated for 30 minutes at 4°C. Cells were washed, pelleted (5 minutes, 1,400 rpm), and resuspended in 250 μL PBS + 5% FBS. One microgram of the secondary antibody, goat anti-human IgG-phycoerythrin (Jackson ImmunoResearch Laboratories), was added and left for 30 minutes at 4°C. Finally, cells were washed, pelleted, and resuspended in 500 μL PBS + 5% FBS for analysis on a Becton Dickinson (San Jose, CA) FACSVantage SE.

Identification of human anti-RON Fab antibodies from a phage display library. A human Fab phage display library containing 3.7×10^{10} clones (39) was used to screen for and identify human anti-RON Fab antibodies following a previously described procedure (40) using RON-Fc (Sigma-Aldrich, St. Louis, MO) as the bait. Individual phage clones recovered after the second and the third round of selections were examined for binding to immobilized RON-Fc by ELISA. Plasmids of individual binders were then used to transform a nonsuppressor *Escherichia coli* host HB2151 for the expression of soluble Fab fragments. The soluble Fab proteins were purified from the bacteria periplasmic extracts by affinity chromatography using a Protein G column, following the protocol of the manufacturer (Amersham Pharmacia Biotech, Piscataway, NJ), and tested for binding to RON-Fc by ELISA.

In MSP/RON blocking assay, Maxi-sorp 96-well microtiter plates (Nunc, Rochester, NY) were coated with MSP (1 μg/mL × 100 μL; R&D Systems, Minneapolis, MN) at room temperature for 1.5 hours. After washing the wells, they were blocked with 3% PBS/milk. Anti-RON antibodies (Fab or full IgG) were preincubated with RON-Fc (25 ng/well) at room temperature for 1 hour. The Fab/RON-Fc or IgG/RON-Fc mixtures were then added to the MSP-coated wells and allowed to incubate for 1.5 hours at room temperature. After several washes, a 1:1,000 dilution of the antihuman IgG, Fab-specific horseradish peroxidase (HRP)–conjugated antibody was added to the plates for 1.5 hours at room temperature to detect the anti-RON Fab or IgG that bound to RON but did not block the MSP/RON interaction. IMC-41A10 and IMC-42E12 are examples of antibodies that blocked and failed to block the MSP/RON interaction, respectively.

ELISA to detect binding of IMC-41A10 to RON. Standard ELISA plates were coated overnight at 4°C with recombinant human MSPR (R&D Systems) at 100 ng/well. The plates were washed once with 0.2% PBS/T and blocked with 3% milk (150 μL/well) for 1 hour at 37°C. Following a wash with 0.2% PBS/T, a 3 nmol/L solution of IMC-41A10 was prepared in 1 mL 3% milk and diluted 1:2 across plates. The plates were incubated for 1 hour at room temperature on a rocker and washed five times with 0.2% PBS/T. The secondary antibody (goat anti-human Fc, HRP-conjugated) was added at 1:5,000 dilution and allowed to incubate for 1 hour at room temperature. Washing was done as above. One hundred microliters of substrate were added per well until a yellow color developed. The reaction was stopped with 50 μL of 1 N H_2SO_4 and the absorbance at 450 nm determined with a standard plate reader.

To determine whether IMC-41A10 could cross-react with c-MET [hepatocyte growth factor receptor (HGFR)], an ELISA was done exactly as described above with the exception that a recombinant human HGFR (c-MET)/Fc chimeric protein (R&D Systems) was used to coat the plates and a mouse anti-human HGFR antibody (R&D Systems) was used as a positive control. A goat anti-mouse HRP antibody was used as the secondary antibody for the positive control.

ELISA to detect IMC-41A10 blocking of MSP binding to RON. ELISA plates were coated with 100 ng/well carrier-free MSP (R&D Systems) overnight at 4°C on a rocker. The plate was washed once with 0.2% PBS/T and blocked for 2 hours at 37°C with 150 μL/well 3% milk. A 15 μg/mL dilution of IMC-41A10 was prepared and serially diluted across another ELISA plate. To the IMC-41A10, we added 100 ng/well recombinant human MSPR (R&D Systems). The IMC-41A10/rh-MSPR complex was allowed to form for 2 hours at room temperature on a rocker. Next, the MSP-coated ELISA plate was washed once with 0.2% PBS/T and 100 μL of the IMC-41A10/rh-MSPR complex were added per well. After a 1.5-hour incubation at room temperature, the plate was washed five times with 0.2% PBS/T and incubated for 1 hour at room temperature with a 1:2,000 dilution of anti–His-tag HRP antibody (Sigma), which recognizes a His tag on the recombinant human MSPR protein. The plate was washed five times with 0.2% PBS/T and 100-μL substrate was added per well until a yellow color developed. The reaction was stopped with 50 μL of 1 N H_2SO_4 and the absorbance at 450 nm determined with a standard plate reader.

Analysis of MSP-induced phosphorylation of RON, mitogen-activated protein kinase, and AKT. Cells were grown in six-well plates or 10-cm dishes to ~70% confluency and serum starved for 18 hours. For cells receiving antibody, 100 nmol/L 41A10 or 42E12 was added and incubated at 37°C for 1 hour. MSP (R&D Systems) was then added to the appropriate cells at 10 nmol/L and incubated for 30 minutes at 37°C. Cells were washed twice with ice-cold PBS and lysates prepared in ice-cold cell extraction buffer (Biosource International, Carlsbad, CA) plus fresh HALT protease inhibitor cocktail (Pierce, Rockford, IL) and 15 μg of lysates were resolved by SDS-PAGE using 4% to 12% NuPAGE Novex Bis-Tris Gels with 1× MOPS running buffer. For Western blotting, proteins were transferred to a nitrocellulose membrane (Invitrogen, Carlsbad, CA) and blocked with 5% nonfat milk in TBS/0.1% Tween 20 (TBS-T) for 1 hour at room temperature on a rocker. After three 5-minute washes with TBS-T, the membrane was incubated with 1:1,000 rabbit polyclonal phospho-p44/42 MAPK (Thr^{202}/Tyr^{204}) antibody (Cell Signaling, Danvers, MA) diluted in 1% nonfat milk in TBS-T or 1:500 rabbit polyclonal anti-phospho-AKT ($P\text{-}Ser^{472/473/474}$) antibody (BD PharMingen, San Jose, CA) or 1:1,000 rabbit monoclonal phosphor-AKT (Ser^{473}) antibody (Cell Signaling). Following three 5-minute washes with TBS-T, a 1:5,000 dilution of anti-rabbit IgG, HRP-conjugated secondary antibody (Amersham) was added to the membrane for 1 hour at room temperature followed by three 5-minute TBS-T washes. Protein bands were detected with Amersham Enhanced Chemiluminescence Western Detection Kit. To determine expression levels of mitogen-activated protein kinase (MAPK), these membranes were stripped with Pierce Restore Western Blot Stripping Buffer (15 minutes at room temperature) and reprobed with a 1:1,000 dilution of p44/42 MAPK polyclonal rabbit antibody (Cell Signaling) or a 1:500 dilution of polyclonal rabbit anti-AKT1 antibody (BD PharMingen) or 1:2,000 rabbit polyclonal anti-AKT antibody (Cell Signaling).

Table 1. RON expression in patient tumor samples as determined by immunohistochemistry analysis of tumor tissue arrays

Cancer tissue	%Positive*	Mean intensity †
Breast	100% (47 of 47)	166 (20-300)
Lung	93% (50 of 54)	142 (15-300)
Prostate	92% (35 of 38)	164 (20-300)
Gastric	73% (38 of 52)	172 (20-300)
Pancreas	69% (36 of 52)	100 (30-200)
Colon	65% (36 of 55)	54 (15-225)

*The percentage of RON-expressing tumor samples on the tumor tissue array is listed. In parentheses, the numerator represents the number of RON-expressing tumor cores and the denominator equals the total number of tumor cores present on the tumor tissue array.
† Mean intensity represents tumor epithelial staining intensity in RON-positive samples. This value is obtained by multiplying a relative intensity score (0-3) by the percentage of epithelial cells present in the sample core. See Materials and Methods for experimental details.

RON-NIH3T3 cells were used to detect MSP-induced phosporylation of RON. The procedure used was exactly as described above with the exception that cells were serum starved for 2.5 hours and stimulated with or without 10 nmol/L MSP for 30 minutes at 37C. Before MSP stimulation, RON antibodies were added to cells for 1 hour at 100 nmol/L to assess blocking activity. To determine whether RON antibodies exhibited agonist activity on RON phosphorylation, antibody was added to cells in the absence of MSP stimulation. Cells were lysed and 30 μg of lysate were resolved on a 4% to 12% gel. Western blot analysis was done with anti-phosphotyrosine antibody, 4G10 (Upstate, Charlottesville, VA), as per recommendation of the manufacturer.

Cell migration assay. To determine whether IMC-41A10 could block the migration of H596 cells induced by MSP, we used cell culture inserts containing porous translucent polyethylene terephthalate track–etched membranes (8.0 μm pore size; Becton Dickinson Falcon). Before the assay, the undersides of the porous membranes in the cell culture inserts were coated with collagen by placing them into a 24-well Falcon plate filled with 700 μL of Vitrogen-100 purified collagen solution (25 μg/mL; Cohesion, Palo Alto, CA). The inserts were left for at least 1 hour at 4°C and placed in a new 24-well plate containing either 700-μL serum-free medium or 10% FBS. Next, 6×10^5 viable cells that had been serum starved for 24 hours were rinsed twice with PBS and seeded into the upper chamber of the cell culture insert in 300 μL of serum-free medium. MSP was added to the lower chamber for 24 hours at 37°C to induce cell adhesion and migration through the collagen-coated porous membrane on the underside of the cell culture insert. Before the addition of MSP, IMC-41A10 was added to other wells to determine if it could inhibit the MSP-induced migration/invasion of H596 cells. IMC-42E12, which binds to RON but does not block MSP binding, was used as a negative control. At the conclusion of the assay, migrated cells present on the underside of the collagen-coated membrane were stained with H&E and visualized by bright field microscopy at ×100 magnification.

***In vitro* "wound" healing assay.** HCA-7 cells were seeded at 2×10^6 in a 4-mL suspension in a 60-mm tissue culture dish and allowed to grow to confluence, refreshing the medium every 3 to 4 days. When 41A10 or anti–keyhole limpet hemocyanin (KLH) antibodies were used, the cells were preincubated with the antibodies for 1 hour before wound infliction. At the start of the assay, a small wound was inflicted with a plastic pipette tip. The cells were incubated for 24 hours with and without the presence of MSP plus anti-KLH or anti-RON (41A10) antibodies. The cells were imaged on a Zeiss microscope immediately after wounding (time 0) and at 16 and 24 hours.

Tumor xenograft models. To establish tumor xenograft models with which to test the antitumor activity of IMC-41A10, 5 million HT-29, NCI-H292, and BXPC-3 cells were mixed with Matrigel (Collaborative Research Biochemicals, Bedford, MA) and s.c. injected into the left flank of 56-week-old female athymic (*nu/nu*) mice (Charles River Laboratories, Wilmington, MA). Tumors were allowed to reach 150 to 300 mm^3 in size and mice were randomized into groups of 12 animals each. Mice were treated by i.p. injection every 3 days with control antibody (human IgG) or IMC-41A10 antibody at a dose of 40 mg/kg or Erbitux at a dose of 40 mg/kg. Treatment of animals was continued for the duration of the study. Tumors were measured twice each week with a caliper and tumor volumes calculated using the following formula: $(\pi/6\ (w_1 \times w_2 \times w_2))$, where w_1 represents the largest tumor diameter, and w_2 represents the smallest tumor.

Analysis of MAPK activity in HT-29 and NCI-H292 tumor xenografts. HT-29 and NCI-H292 tumor xenografts were established as described above with the exception that six mice were used for IMC-41A10 treatment and six used for control IgG treatment. Once tumors reached ~300 mm^3, mice were injected once with an antibody dose of 40 mg/kg. After 24 hours, mice were sacrificed and tumors excised. Tumor lysates were prepared and subjected to Western blot analysis. To determine whether IMC-41A10 had an effect on MAPK activity, phosphorylated and total MAPK levels were detected as described above and subjected to densitometric analysis. The densitometric values for the total MAPK bands were normalized to 20,000 and, in turn, the densitometric values of the phosphorylated MAPK bands were proportionately adjusted. The adjusted phosphorylated MAPK values for the six IMC-41A10 mice were averaged and compared with those of the six control IgG mice. Statistical significance between the two groups was determined by Student's t test.

Results

RON is expressed in several cancerous tissues and cell lines. We did an extensive analysis of RON expression in several cancer tissues by tumor tissue arrays as well as in cell lines by flow cytometry and Western blot analyses. In addition, through access to the Gene Logic Ascenta database, we were able to assess RON expression profile in a variety of cancer tissues as well as in the NCI-60 cancer cell line panel. Table 1 is a summary of RON expression in human cancer as determined by immunohistochemistry of Imgenex tumor tissue arrays. RON was expressed in 100%, 93%, 92%, 73%, 69%, and 65% of breast, lung, prostate, gastric, pancreas, and colon tumors, respectively. Table 1 also shows the mean intensity of RON expression in the tumor epithelial cells for each of these cancer types. Figure 1 is a montage of tumor tissue sections from these tumor tissue arrays that exhibit a mean epithelial cell intensity of RON expression similar to that listed in Table 1. Patient information for the tumor tissue sections shown in Fig. 1 is given in the figure legend. With respect to cancer cell lines, Table 2 lists those that are positive and negative for RON expression on the basis of flow cytometry, Western blotting, and Ascenta data (Gene Logic). Of the ~100 cell lines tested that cover 10 different cancer types, approximately half exhibited RON expression. Interestingly, none of the leukemic and renal cancer cell lines expressed RON by these analyses.

Identification and characterization of IMC-41A10 as an antibody that binds to RON and blocks its interaction with MSP. To determine whether RON plays a functional role in tumor growth, we generated a neutralizing monoclonal antibody. For this task, a human Fab antibody/phage display library was used to isolate fully human high-affinity antibodies capable of binding the RON receptor and blocking ligand binding (data not shown). To begin this process, an Fc fusion protein of the extracellular portion of the RON receptor was used to screen the Fab phage display

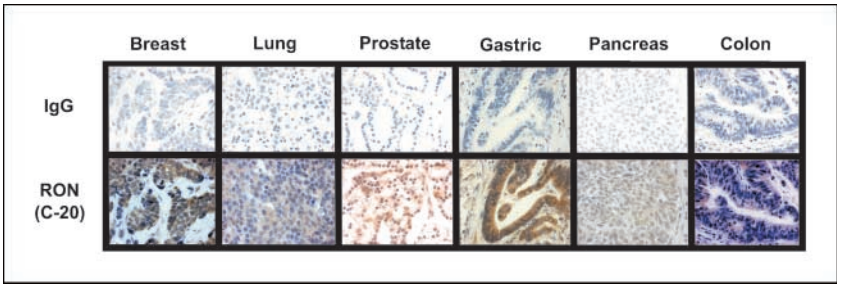

Figure 1. Montage of immunohistochemistry images from the tumor tissue array analysis of RON expression described in Table 1. The images shown in this figure were chosen to match the mean expression intensity of RON reported for each cancer type in Table 1. Patient data corresponding to the tumor images are as follows: Breast (infiltrating ductal carcinoma, stage T_{4b}), Lung (adenosquamous carcinoma, stage IIIA, $T_2N_2M_0$), Prostate (adenocarcinoma, stage III, $T_3N_0M_0$), Gastric (stage IB, $T_2N_0M_0$, well differentiated), Pancreas (ductal adenoma, stage III), and Colon (sigmoid adenocarcinoma, stage II, $T_3N_0M_0$, moderately differentiated).

library, which contains $\sim 10^7$ naïve recombinant Fab fragments. Following three rounds of selection, binding Fab fragments were identified. Four of these were subsequently found to efficiently block the interaction of MSP ligand with RON. Following the cloning of these Fabs into mammalian expression vectors harboring the fully human IgG1 backbone, one antibody, IMC-41A10, was chosen for further studies.

To quantitate the binding and blocking potential of IMC-41A10 to RON, ELISA assays were established. ELISA data revealed a receptor binding ED_{50} of 0.15 nmol/L and a receptor blocking IC_{50} of 2 nmol/L for IMC-41A10 (Fig. 2*A* and *B*). Because RON is a member of the c-MET receptor family, we wanted to determine whether IMC-41A10 could also bind c-MET. Using an ELISA-based binding assay with immobilized soluble extracellular c-MET protein, we showed that IMC-41A10 could not bind c-MET (Fig. 2*C*).

IMC-41A10 significantly inhibits MSP-dependent phosphorylation of RON and downstream signaling. Once IMC-41A10 was shown to function in solid-phase receptor binding and blocking assays, we evaluated its ability to block the activity of the RON receptor and the downstream effectors, MAPK and AKT, in cell-based assays. To assess the ability of IMC-41A10 to inhibit RON phosphorylation, we used NIH3T3 cells overexpressing the recombinant wild-type RON protein (Fig. 3*A*). When these cells were serum starved and stimulated with MSP, tyrosine phosphorylation of RON was readily detected and could be significantly inhibited ($\sim$75%) by the addition of IMC-41A10. In contrast, no inhibition of RON phosphorylation was noted with IMC-42E12 (an antibody that binds to RON but does not block MSP binding to RON). It is important to note that when 41A10 was added to the RON-NIH3T3 cells in the absence of MSP (Fig. 3*A, lane 3*), no induction of RON phosphorylation was observed, indicating that IMC-41A10 is devoid of agonist activity on the RON receptor. Because the MSP/RON pathway is known to affect MAPK and AKT activity, we were interested in evaluating the potential of IMC-41A10 to inhibit the phosphorylation and subsequent activation of MAPK (Fig. 3*B*). Using cell lines that represent a number of different cancers [i.e., HT-29 (colon), NCI-H292 (lung), HCC-1937 (breast), BXPC-3 (pancreas), DU145 (prostate), and AGS (gastric)], we determined that IMC-41A10 was able to completely inhibit MSP-induced phosphorylation of MAPK in every case and of AKT in HT-29, DU145, and AGS cells. Following MSP treatment, AKT phosphorylation did not occur in NCI-H292, BXPC-3 and HCC-1937 cells. It is also interesting to note that for many of the aforementioned cell lines, constitutive phosphorylation of MAPK and AKT was noted in the absence of exogenously added MSP.

IMC-41A10 significantly inhibits cell migration. Like HGF and c-MET, MSP and RON have been implicated in the migration and invasion of certain macrophage and epithelial cells. Previously, MSP was shown to induce migration of the H596 lung cancer cell line *in vitro* (14). We modified this assay (Fig. 4*A*) and tested the

Table 2. Flow cytometric, Western blot, and Gene Logic analyses of RON expression in cancer cell lines

Tumor type	Positive cell lines	Negative cell lines
Colon	DiFi, HCT-8, HCT-15, HCT-116 HCC-2998, Colo205, Colo-201 DLD-1, GEO, T84, HT-29, KM12 Sw480, Sw620	SNU-C1, LoVo, CaCo-2
Lung	NCI-H1650, NCI-H292, NCI-H1975, NCI-H358, NCI-H1666, NCI-H226, NCI-H441, NCI-H1650, NCI-H727, NCI-H596, NCI-H322M, EKVX, A549	NCI-H460, NCI-H23, NCI-H522 Hop-62, Hop-92
Pancreas	BXPC-3, Capan-2, HPAC, HPAFII L3#7.p1, Hs766.T, ASPC-1, CFPAC-1	MIA-PACA-2
Breast	T47D, HCC-1937, MDA-MB-468, BT20, DU4475	MDA-MB-231, MDA-MB-435, MCF-7, BT-474, SKBR3, Hs578T
Ovary	SKOV3, OVCAR3, OVCAR5, MDAH-2774, IGOV-1, OV90	OVCAR8, CaCOV3, CaCOV4
Prostate	PC-3, DU145, LnCAP	22RV.1
Stomach	NCI-N87, AGS	SNU-1, SNU-16, KKVR
Liver	HepG2	SNU-182, SNU-449, SNU-475 SNU-398, Hep3B, PLC/PRF/5
Leukemia		EOL, JM-1, HEL, Jurkat, TF-1 U937, HL-60
Kidney		A498, Caki-1, SKRC29, 786-0, ACHN, RXF-393, SN12C, TK-10, UO-31

NOTE: Of the cell lines present in the NCI-60 cancer cell line panel, expression analysis was collected from Gene Logic's Ascenta database, which contains Affymetrix expression data for the NCI-60 cancer cell line panel. These data were accessed through an institutional subscription to the Ascenta database.

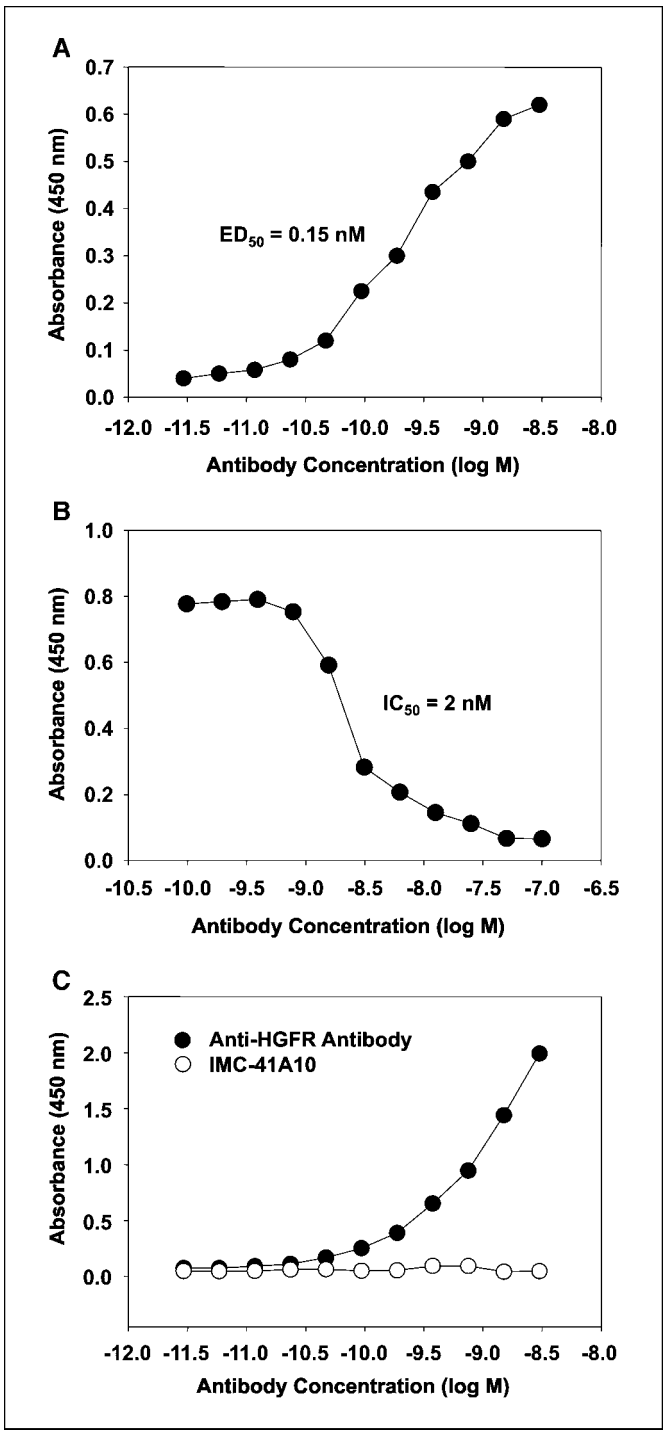

Figure 2. Solid-phase binding and blocking characteristics of IMC-41A10. *A,* ELISA to determine the ED_{50} of IMC-41A10 binding to immobilized rh RON protein. *B,* ELISA to determine the IC_{50} of IMC-41A10 needed to block the interaction of recombinant human MSP to immobilized recombinant human RON protein. *C,* ELISA to determine whether IMC-41A10 can bind to immobilized recombinant human c-MET protein. An antihuman HGFR (c-MET) antibody is used as a positive control.

ability of IMC-41A10 to inhibit MSP-induced migration of H596 cells. In comparison with IMC-42E12, IMC-41A10 showed >90% inhibition of MSP-mediated cell migration (Fig. 4*B*). These data are shown graphically in Supplementary Fig. S1. Using an *in vitro* wound healing assay, we also showed that IMC-41A10 could significantly inhibit (~75%) the ability of HCA7 colon cancer cells to migrate in response to MSP and close a "wound" created in their monolayer (Fig. 4*C*). Taken together, these data confirm that MSP-dependent tumor cell migration can be inhibited by antagonizing MSP binding to RON.

IMC-41A10 possesses antitumor activity. Because IMC-41A10 successfully abrogated RON signaling and cell migration/invasion, we were interested in determining whether it could inhibit tumorigenicity. To begin to test the antitumor activity of IMC-41A10, murine tumor xenograft models were established using HT-29 colon, NCI-H292 lung, and BXPC-3 pancreatic cancer cells. These cells were s.c. injected into nude mice and tumors allowed to establish to a size of ~250 mm^3 before being randomized into treatment groups. IMC-41A10 and a control human IgG were subsequently injected i.p. at a dose of 40 mg/kg every 3 days. In comparison with control IgG-injected mice, IMC-41A10 treatment led to a 58%, 50%, and 50% inhibition of HT-29, NCI-H292, and BXPC-3 tumor growth, respectively (Fig. 5*A-C*). It should be noted that no differences in tumor necrosis were observed in control IgG versus IMC-41A10-treated tumors (see Supplementary Fig. S2 for examples of HT-29 tumor xenografts).

To determine whether IMC-41A10 could be more efficacious in HT-29 xenografts, we initiated a subcutaneous prophylactic murine tumor xenograft model where IMC-41A10 was administered at 40 and 80 mg/kg every 3 days commencing 1 day after HT-29 cells were injected (Supplementary Fig. S3). IMC-41A10 did not exhibit increased efficacy in this model versus the established subcutaneous HT-29 tumor xenograft model in Fig. 5*A*.

IMC-41A10 inhibits phosphorylation of MAPK in HT-29 and NCI-H292 tumor xenografts. Because IMC-41A10 was shown to inhibit MAPK phosphorylation in cultured HT-29 and NCI-H292 cells (Fig. 3), we were interested in confirming whether MAPK signaling was also inhibited in xenograft tumors of IMC-41A10-treated mice. After treating established HT-29 and NCI-H292 tumors with a single 40 mg/kg dose of IMC-41A10, tumor lysates were prepared after 24 and 72 hours, respectively, to quantitate MAPK phosphorylation levels by Western blot analysis. We found that IMC-41A10 treatment of HT-29 and NCI-H292 xenografts resulted in a 35% and 28% mean decrease in phosphorylated MAPK levels compared with control IgG-treated tumors (Fig. 6). IMC-41A10-treated HT-29 tumors 2, 4, and 5 as well as NCI-H292-treated tumors 1, 2, and 4 showed phosphorylated MAPK levels below that of any of the IgG-treated tumors. With the exception of the IMC-41A10-treated NCI-H292 tumor 3, none of the IMC-41A10-treated tumors exhibited higher phosphorylated MAPK levels than the highest control IgG-treated tumors, a finding which also shows that IMC-41A10 is devoid of agonist activity. Taken together, these data show that treatment of tumor xenografts with IMC-41A10 led to a significant inhibition of tumor growth via inhibition of RON-dependent signaling in tumor cells.

Discussion

A substantial body of evidence exists to support a functional role for c-MET in human cancer (2). In addition, several c-MET receptor antagonists have shown antitumor activity in animal models, thereby implicating c-MET as a potential target for therapeutic intervention (2). In comparison with c-MET, RON has not been as extensively studied. Within the last few years, however, data have accumulated to suggest that not only is RON expressed in several cancers but it also may play a functional role in tumor formation.

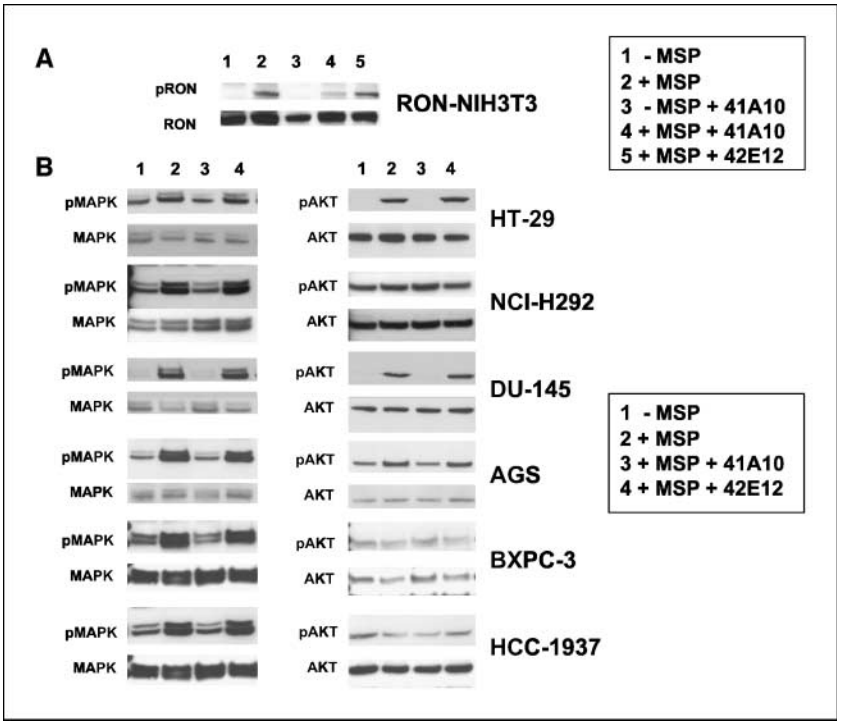

Figure 3. Inhibition of MSP-dependent receptor and MAPK phosphorylation. *A,* effect of IMC-41A10 on MSP-induced phosphorylation of RON. RON-NIH3T3 cells were serum starved (*lane 1*) and stimulated with MSP (*lanes 2, 4*, and *5*). *Lanes 3* and *4,* effect of adding IMC-41A10 in the absence and presence of MSP, respectively. *Lane 5,* effect of adding IMC-42E12, an antibody that binds to RON but does not block MSP binding, in the presence of MSP. *B,* effect of IMC-41A10 on MSP-induced phosphorylation of MAPK in cell lines representing six types of cancer. These lines were serum starved (*lane 1*) and stimulated with MSP (*lane 2*). *Lanes 3* and *4,* effect of adding IMC-41A10 in comparison with IMC-42E12, respectively.

Although RON antagonists have been reported (41–44), to our knowledge, none have been tested for antitumor activity to validate RON as a potential cancer target. Consequently, we developed IMC-41A10, a fully human IgG1 antibody that binds to human RON with high affinity (ED_{50} = 0.15 nmol/L) and blocks interaction with its ligand, MSP (IC_{50} = 2 nmol/L). IMC-41A10 does not bind to c-MET and possesses no agonist activity.

Whereas other neutralizing antibodies have been reported for RON (42), IMC-41A10 represents the first RON antibody to show antitumor activity. As a single agent, IMC-41A10 showed 50% to 60% inhibition of established tumor growth in three s.c. xenograft models using HT-29 colon, NCI-H292 lung, and BXPC-3 pancreatic cancer cells. We hypothesize that the reason IMC-41A10 treatment alone did not lead to tumor growth stabilization or regression in these three cell lines is because pathways in addition to RON are required for their tumorigenicity. Consistent with this notion is the fact that when IMC-41A10 treatment was given in combination with Erbitux (an anti-EGFR antibody) in BXPC-3 xenografts, tumor regression was observed in 5 of 12 mice. In contrast, although IMC-41A10 and Erbitux significantly inhibited BXPC-3 tumor growth, neither antibody, on its own, led to tumor growth stabilization or regression. In the future, it will be important to determine whether enhanced tumor inhibition will result following combination treatment with other antibodies or targeted therapies as well

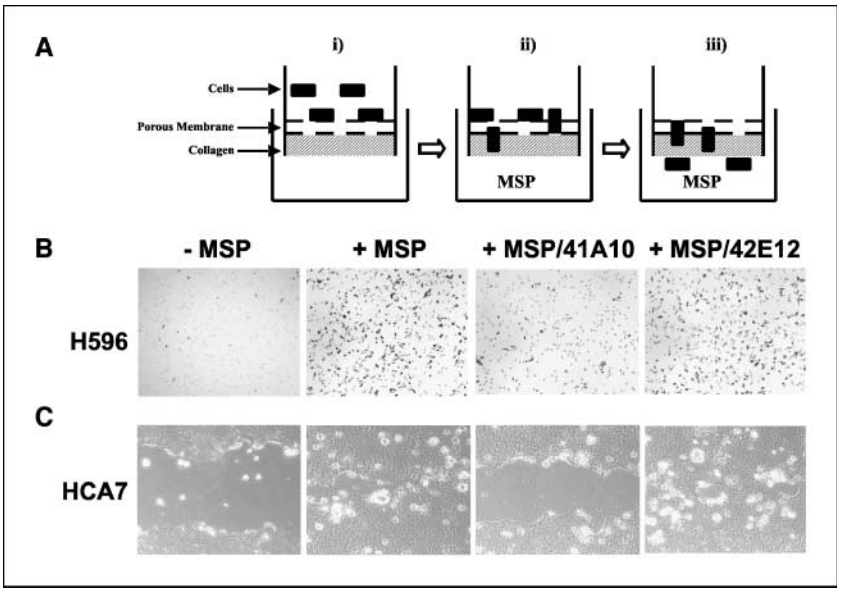

Figure 4. Ability of IMC-41A10 to inhibit cell migration. *A,* schematic of cell migration assay. *i,* cells are placed in the upper chamber of a cell culture insert and lowered into a well of a 24-well plate containing serum-free medium. The cell culture insert contains a porous membrane with collagen coated on its underside. After 24 hours, fresh serum-free medium containing MSP ± antibody is added to the lower chamber (*ii*) and cells migrate through the porous membrane and collagen and adhere to the underside of the collagen (*iii*). *B,* H&E staining of H596 lung cancer cells that have adhered to and migrated through to the underside of the collagen in the presence of IMC-41A10 and IMC-42E12, an antibody that binds to RON but does not block MSP binding. *C, in vitro* wound healing assay. A scratch was made in a monolayer of HCA7 colon cancer cells. IMC-41A10 was added to determine whether it could inhibit the ability of MSP to induce the migration of cells to fill the wound.

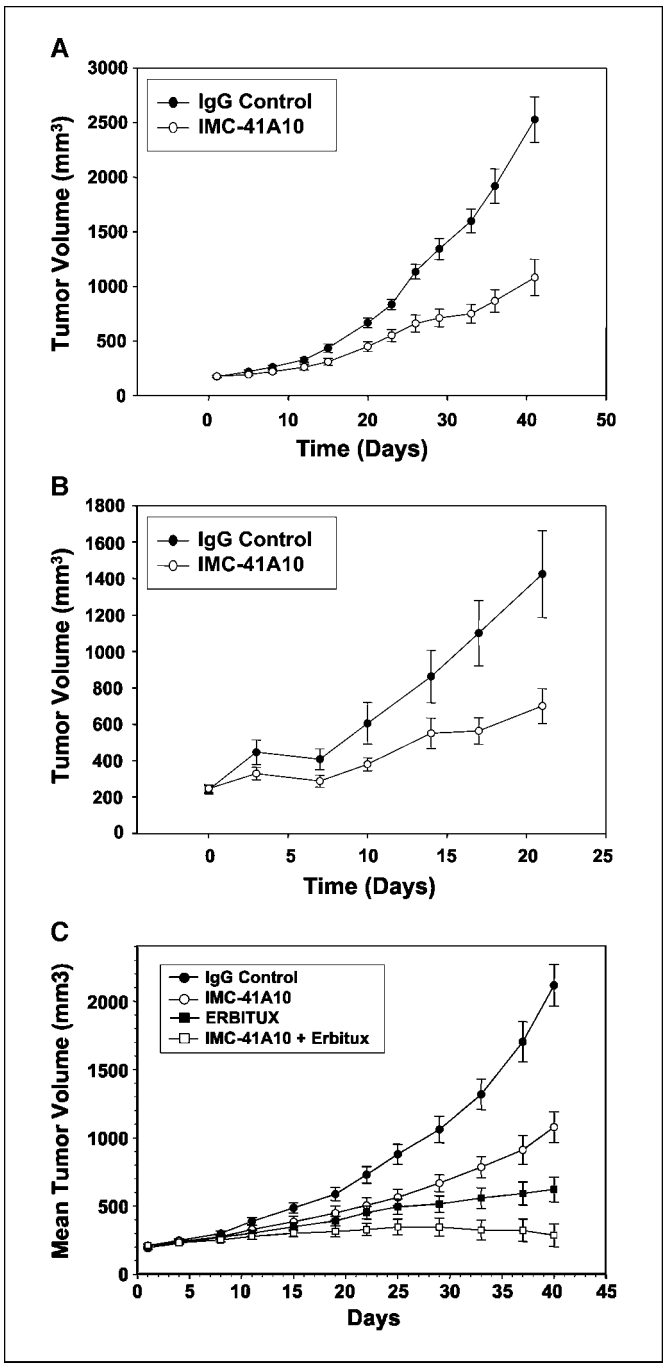

Figure 5. IMC-41A10 inhibits the growth of tumor xenografts in nude mice. HT-29 colon (*A*), NCI-H292 lung (*B*), and BXPC-3 pancreatic (*C*) cancer cells were injected s.c. into nude mice and allowed to grow to ~250 mm^3. Groups of 12 mice each were treated i.p. with 40 mg/kg of control human IgG or IMC-41A10 every 3 days. BXPC-3 xenograft tumor-bearing mice were also i.p. treated with Erbitux or the combination of Erbitux and IMC-41A10, each administered at 40 mg/kg every 3 days. Tumor size was measured with a caliper at regular intervals. *Bars,* SE. Statistical significance was determined by Student's *t* test.

as with various forms of chemotherapy and radiation. Testing the efficacy of IMC-41A10 in other subcutaneous as well as orthotopic tumor xenograft models will also be of interest.

Interestingly, IMC-41A10 inhibition of RON activity and tumorigenicity in HT-29 cells is consistent with the work of Xu et al. (31) who showed that repression of RON expression in HT-29 cells by RNA interference caused a decrease in cell proliferation and an increase in apoptosis. HT-29 cells have been shown to express constitutively active splice variants of RON with small deletions in the extracellular portion that possess enhanced oncogenic potential (26–28). Whereas we have not determined whether IMC-41A10 can interact with these constitutively active oncogenic RON variants, it is noteworthy that IMC-41A10 showed strong antitumor activity in HT-29 cells that express wild-type RON in addition to the splice variants.

Despite the fact that IMC-41A10 cross-reacts with murine RON (data not shown), no adverse effects were noted during treatment of tumor-bearing mice in this study. Thus, it seems that toxicity is not associated with inhibition of murine RON activity. This is an important finding given the phenotype of RON knockout mice and the role that RON is thought to play in normal inflammatory cells as a potential negative regulator of inflammation (8, 9).

To investigate the antitumor activity of IMC-41A10, we considered ligand-dependent and -independent mechanisms. With regard to the former, we evaluated whether IMC-41A10 could modulate MSP-dependent MAPK and AKT activation as well as cell migration.

Like HGF, it is well established that MSP (HGF-like protein) affects cell migration/invasion. Moreover, it is believed that cancer cells expressing c-MET or RON are prone to tissue invasion and metastasis (2, 3, 25). Using two *in vitro* cell migration assays, we showed IMC-41A10 to be a potent inhibitor of MSP-induced cell migration in H596 lung and HCA7 colon cancer cells. In the future, it will be of interest to determine whether IMC-41A10 will show efficacy in *in vivo* tumor metastasis models using these and other cell lines.

MAPK and AKT are known to be key downstream effector molecules governing a variety of cellular pathways respectively associated with cell growth and survival. Because MAPK and AKT have been shown to be modulated by RON receptor signaling (12), we were keen to discover whether IMC-41A10 could inhibit their phosphorylation and subsequent activation. We found IMC-41A10 to be a potent inhibitor of MSP-induced phosphorylation of MAPK *in vitro* in HT-29 cells as well as in cultured NCI-H292, DU145, AGS, BXPC-3, and HCC-1937 cells, which represent lung, prostate, gastric, pancreatic, and breast cancer, respectively. IMC-41A10 also proved to be a potent inhibitor of AKT phosphorylation in HT-29, DU145, and AGS cells. In HT-29 and NCI-H292 tumor xenografts treated with IMC-41A10 for 24 and 72 hours, respectively, we observed a 35% and 28% inhibition of MAPK phosphorylation following a single treatment. Because IMC-41A10 treatment of HT-29 and NCI-H292 tumor xenografts occurred for several weeks, it is reasonable to assume that the cumulative effect of IMC-41A10 treatment on MAPK activity would be to significantly and negatively affect tumor growth. Because HT-29 and NCI-H292 cells do not produce MSP (Supplementary Fig. S4) but are sensitive to MSP stimulation *in vitro*, our data suggest not only that *in vivo* activation of MAPK in these cell lines is mediated by paracrine stimulation of the RON receptor with murine MSP but also that IMC-41A10 effectively inhibits the murine MSP-RON interaction. Taken together, the inhibitory effects of IMC-41A10 on MAPK and AKT phosphorylation would suggest not only a negative effect on cell growth and survival but may also be predictive of the antitumor potential of IMC-41A10 treatment in cancer cell lines where it modulates phosphorylation of MAPK and AKT. With respect to MSP-independent mechanisms of tumor inhibition, we did experiments to test whether IMC-41A10 treatment led to (*a*)

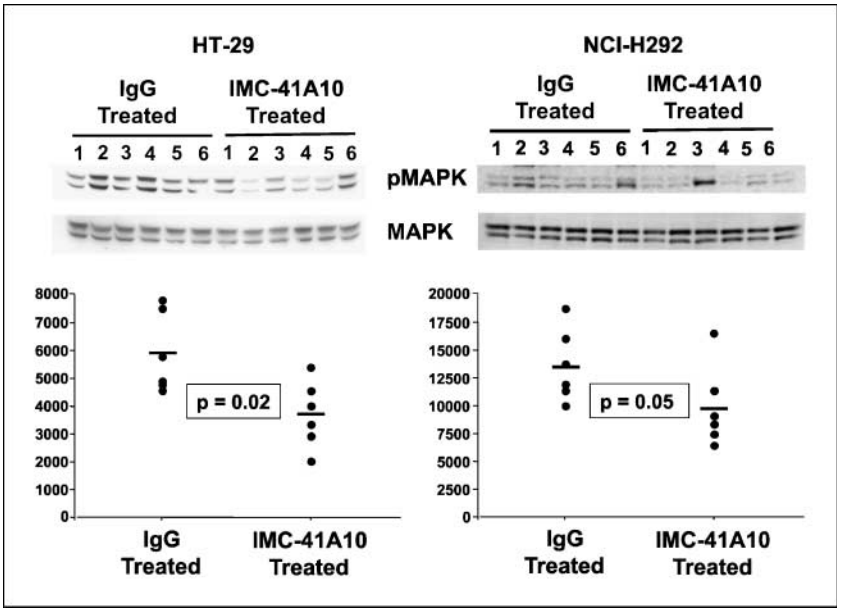

Figure 6. IMC-41A10 inhibits phosphorylation of MAPK in HT-29 and NCI-H292 tumor xenografts. HT-29 and NCI-H292 cells were s.c. injected into 24 nude mice and allowed to reach ~300 mm^3. For each cell line, six mice were treated with IMC-41A10 and six with control IgG. Twenty-four hours (HT-29) and 72 hours (NCI-H292) after a single injection with antibody at a dose of 40 mg/kg, tumors were excised and lysates prepared for Western blot analysis to detect MAPK and phosphorylated MAPK levels. Densitometric values for total MAPK bands were normalized to 20,000 and, in turn, the densitometric values of the phosphorylated MAPK bands were proportionately adjusted. The adjusted phosphorylated MAPK values for IMC-41A10-treated mice were averaged and compared with those of the control IgG-treated mice. Statistical significance between the two groups was determined by Student's *t* test.

RON receptor down-regulation (Supplementary Fig. S5*A* and *B*); (*b*) repression of vascular endothelial growth factor secretion (Supplementary Fig. S6*A*); (*c*) induction of apoptosis (Supplementary Fig. S6*B*); and (*d*) induction of complement-dependent cytotoxic or antibody-dependent cell-mediated cytotoxic activity (Supplementary Fig. S7*A* and *B*). Whereas results from these experiments were conclusive, they were also negative and did not suggest an MSP-independent mechanism of action for the antitumor activity of IMC-41A10. With respect to the inability of IMC-41A10 to elicit complement-dependent cytotoxic and antibody-dependent cell-mediated cytotoxic activities on cell lines tested, we emphasize that it is possible that IMC-41A10 (a human IgG1 antibody) could elicit such activity *in vivo*. Furthermore, we stress that other MSP-independent mechanisms may contribute to the antitumor efficacy of IMC-41A10 but await further experimentation.

Whereas some reports exist that provide evidence for RON expression in human tumors, the number of patients was not always sufficient and methods used to examine expression were varied. In this report, we conducted an extensive systematic analysis of RON expression in ~100 cancer cell lines representing 10 cancer types and in 6 different tumor types using commercial tumor tissue arrays harboring nearly 300 individual tumor samples. RON was expressed in approximately half of the cell lines and was expressed by at least one cell line per cancer type with the exception of the leukemic and renal cancer cell lines tested. With respect to the tumor tissue array results, RON was well expressed in every cancer type (breast, 100%; lung, 93%; prostate, 92%; gastric, 73%; pancreas, 69%; and colon, 65%). We observed no significant correlation between the extent of RON expression and the stage or severity of disease. These results make a significant contribution to the expression profile of RON in a variety of tumor tissues and cancer cell lines.

In conclusion, our data show that not only is RON well expressed in several cancers but it is also an "inhibitable" target that contributes to tumorigenesis. Our findings also underscore the potential of using an antibody to antagonize RON activity for the treatment of human cancers such as colon, lung, pancreas, and probably other cancers.

Acknowledgments

Received 1/24/2006; revised 6/7/2006; accepted 7/12/2006.

The costs of publication of this article were defrayed in part by the payment of page charges. This article must therefore be hereby marked *advertisement* in accordance with 18 U.S.C. Section 1734 solely to indicate this fact.

We thank Cellestan for pathologic analyses of our tumor tissue array data; Chris Damoci, Deevi Dhanvanthri, and Jim Tonra for animal work; and Anthony Kayas, Mary Amasia, Xenia Jimenez, and Dave Sargent for assistance with antibody production, purification, and characterization studies. Dedication: ILU-MdLSP-RIP.

References

1. Ronsin C, Muscatelli F, Mattei MG, Breathnach R. A novel putative receptor protein tyrosine kinase of the met family. Oncogene 1993;8:1195–202.
2. Christensen JG, Burrows J, Salgia R. c-Met as a target for human cancer and characterization of inhibitors for therapeutic intervention. Cancer Lett 2005;225:1–26.
3. Camp ER, Liu W, Fan F, Yang A, Somcio R, Ellis LM. RON, a tyrosine kinase receptor involved in tumor progression and metastasis. Ann Surg Oncol 2005;12:273–81.
4. Leonard EJ, Danilkovitch A. Macrophage stimulating protein. Adv Cancer Res 2000;77:139–67.
5. Chen YQ, Fisher JH, Wang MH. Activation of the RON receptor tyrosine kinase inhibits inducible nitric oxide synthase (iNOS) expression by murine peritoneal exudate macrophages: phosphatidylinositol-3 kinase is required for RON-mediated inhibition of iNOS expression. J Immunol 1998;161:4950–9.
6. Wang MH, Fung HL, Chen YQ. Regulation of the RON receptor tyrosine kinase expression in macrophages: blocking the RON gene transcription by endotoxin-induced nitric oxide. J Immunol 2000;164:3815–21.
7. Zhou YQ, Chen YQ, Fisher JH, Wang MH. Activation of the RON receptor tyrosine kinase by macrophage-stimulating protein inhibits inducible cyclooxygenase-2 expression in murine macrophages. J Biol Chem 2002; 277:38104–10.
8. Leonis MA, Toney-Earley K, Degen SJ, Waltz SE. Deletion of the Ron receptor tyrosine kinase domain in mice provides protection from endotoxin-induced acute liver failure. Hepatology 2002;36:1053–60.
9. Wang MH, Zhou YQ, Chen YQ. Macrophage-stimulating protein and RON receptor tyrosine kinase: potential regulators of macrophage inflammatory activities. Scand J Immunol 2002;56:545–53.
10. Chen YQ, Zhou YQ, Wang MH. Activation of the RON receptor tyrosine kinase protects murine macrophages from apoptotic death induced by bacterial lipopolysaccharide. J Leukoc Biol 2002;71:359–66.
11. Wang MH, Dlugosz AA, Sun Y, Suda T, Skeel A, Leonard EJ. Macrophage-stimulating protein induces

proliferation and migration of murine keratinocytes. Exp Cell Res 1996;226:39–46.
12. Danilkovitch-Miagkova A. Oncogenic signaling pathways activated by RON receptor tyrosine kinase. Curr Cancer Drug Targets 2003;3:31–40.
13. Chen YQ, Zhou YQ, Angeloni D, Kurtz AL, Qiang XZ, Wang MH. Overexpression and activation of the RON receptor tyrosine kinase in a panel of human colorectal carcinoma cell lines. Exp Cell Res 2000;261:229–38.
14. Willett CG, Wang MH, Emanuel RL, et al. Macrophage-stimulating protein and its receptor in non-small-cell lung tumors: induction of receptor tyrosine phosphorylation and cell migration. Am J Respir Cell Mol Biol 1998;18:489–96.
15. Maggiora P, Marchio S, Stella MC, et al. Overexpression of the RON gene in human breast carcinoma. Oncogene 1998;16:2927–33.
16. Lee WY, Chen HH, Chow NH, Su WC, Lin PW, Guo HR. Prognostic significance of co-expression of RON and MET receptors in node-negative breast cancer patients. Clin Cancer Res 2005;11:2222–8.
17. Okino T, Egami H, Ohmachi H, et al. Immunohistochemical analysis of distribution of RON receptor tyrosine kinase in human digestive organs. Dig Dis Sci 2001;46:424–9.
18. Maggiora P, Lorenzato A, Fracchioli S, et al. The RON and MET oncogenes are co-expressed in human ovarian carcinomas and cooperate in activating invasiveness. Exp Cell Res 2003;288:382–9.
19. Cheng HL, Liu HS, Lin YJ, et al. Co-expression of RON and MET is a prognostic indicator for patients with transitional-cell carcinoma of the bladder. Br J Cancer 2005;92:1906–14.
20. Chen Q, Seol DW, Carr B, Zarnegar R. Co-expression and regulation of Met and Ron proto-oncogenes in human hepatocellular carcinoma tissues and cell lines. Hepatology 1997;26:59–66.
21. Rampino T, Gregorini M, Soccio G, et al. The Ron proto-oncogene product is a phenotypic marker of renal oncocytoma. Am J Surg Pathol 2003;27:779–85.
22. Patton KT, Tretiakova MS, Yao JL, et al. Expression of RON proto-oncogene in renal oncocytoma and chromophobe renal cell carcinoma. Am J Surg Pathol 2004;28:1045–50.
23. Peace BE, Hill KJ, Degen SJ, Waltz SE. Cross-talk between the receptor tyrosine kinases Ron and epidermal growth factor receptor. Exp Cell Res 2003;289:317–25.
24. Follenzi A, Bakovic S, Gual P, Stella MC, Longati P, Comoglio PM. Cross-talk between the proto-oncogenes Met and Ron. Oncogene 2000;19:3041–9.
25. Tamagnone L, Comoglio PM. Control of invasive growth by hepatocyte growth factor (HGF) and related scatter factors. Cytokine Growth Factor Rev 1997;8:129–42.
26. Wang MH, Wang D, Chen YQ. Oncogenic and invasive potentials of human macrophage-stimulating protein receptor, the RON receptor tyrosine kinase. Carcinogenesis 2003;24:1291–300.
27. Zhou YQ, He C, Chen YQ, Wang D, Wang MH. Altered expression of the RON receptor tyrosine kinase in primary human colorectal adenocarcinomas: generation of different splicing RON variants and their oncogenic potential. Oncogene 2003;22:186–97.
28. Peace BE, Hughes MJ, Degen SJ, Waltz SE. Point mutations and overexpression of Ron induce transformation, tumor formation, and metastasis. Oncogene 2001;20:6142–51.
29. Chen YQ, Zhou YQ, Fisher JH, Wang MH. Targeted expression of the receptor tyrosine kinase RON in distal lung epithelial cells results in multiple tumor formation: oncogenic potential of RON *in vivo*. Oncogene 2002;21:6382–6.
30. Chen YQ, Zhou YQ, Fu LH, Wang D, Wang MH. Multiple pulmonary adenomas in the lung of transgenic mice overexpressing the RON receptor tyrosine kinase, Recepteur d'origine nantais. Carcinogenesis 2002;23:1811–9.
31. Xu XM, Wang D, Shen Q, Chen YQ, Wang MH. RNA-mediated gene silencing of the RON receptor tyrosine kinase alters oncogenic phenotypes of human colorectal carcinoma cells. Oncogene 2004;23:8464–74.
32. Santoro MM, Collesi C, Grisendi S, Gaudino G, Comoglio PM. Constitutive activation of the RON gene promotes invasive growth but not transformation. Mol Cell Biol 1996;16:7072–83.
33. Wang MH, Kurtz AL, Chen Y. Identification of a novel splicing product of the RON receptor tyrosine kinase in human colorectal carcinoma cells. Carcinogenesis 2000;21:1507–12.
34. Okino T, Egami H, Ohmachi H, et al. Presence of RON receptor tyrosine kinase and its splicing variant in malignant and non-malignant human colonic mucosa. Int J Oncol 1999;15:709–14.
35. Collesi C, Santoro MM, Gaudino G, Comoglio PM. A splicing variant of the RON transcript induces constitutive tyrosine kinase activity and an invasive phenotype. Mol Cell Biol 1996;16:5518–26.
36. Peace BE, Toney-Earley K, Collins MH, Waltz SE. Ron receptor signaling augments mammary tumor formation and metastasis in a murine model of breast cancer. Cancer Res 2005;65:1285–93.
37. Chan EL, Peace BE, Collins MH, Toney-Earley K, Waltz SE. Ron tyrosine kinase receptor regulates papilloma growth and malignant conversion in a murine model of skin carcinogenesis. Oncogene 2005;24:479–88.
38. Burtrum D, Zhu Z, Lu D, et al. A fully human monoclonal antibody to the insulin-like growth factor I receptor blocks ligand-dependent signaling and inhibits human tumor growth *in vivo*. Cancer Res 2003;63:8912–21.
39. Hoet RM, Cohen EH, Kent RB, et al. Generation of high-affinity human antibodies by combining donor-derived and synthetic complementarity-determining-region diversity. Nat Biotechnol 2005;23:344–8.
40. Lu D, Jimenez X, Zhang H, Bohlen P, Witte L, Zhu Z. Selection of high affinity human neutralizing antibodies to VEGFR2 from a large antibody phage display library for antiangiogenesis therapy. Int J Cancer 2002;97:393–9.
41. Bardelli A, Longati P, Williams TA, Benvenuti S, Comoglio PM. A peptide representing the carboxyl-terminal tail of the met receptor inhibits kinase activity and invasive growth. J Biol Chem 1999;274:29274–81.
42. Montero-Julian FA, Dauny I, Flavetta S, et al. Characterization of two monoclonal antibodies against the RON tyrosine kinase receptor. Hybridoma 1998;17:541–51.
43. Angeloni D, Danilkovitch-Miagkova A, Miagkov A, Leonard EJ, Lerman MI. The soluble sema domain of the RON receptor inhibits macrophage-stimulating protein-induced receptor activation. J Biol Chem 2004;279:3726–32.
44. Matzke A, Herrlich P, Ponta H, Orian-Rousseau V. A five-amino-acid peptide blocks Met- and Ron-dependent cell migration. Cancer Res 2005;65:6105–10.

Therapeutic Implications of a Human Neutralizing Antibody to the Macrophage-Stimulating Protein Receptor Tyrosine Kinase (RON), a c-MET Family Member

Jennifer M. O'Toole, Karen E. Rabenau, Kerri Burns, et al.

Cancer Res 2006;66:9162-9170.